

This is the peer reviewed version of the following article:

Filling the Gap in the Classification of Phlogopite-Bearing Ultramafic Rocks / Giovanardi, Tommaso; Freddo, Ivan; Mazzucchelli, Maurizio. - In: THE JOURNAL OF GEOLOGY. - ISSN 0022-1376. - 126:3(2018), pp. 361-370. [10.1086/697244]

*Terms of use:*

The terms and conditions for the reuse of this version of the manuscript are specified in the publishing policy. For all terms of use and more information see the publisher's website.

18/12/2025 19:33

# The Journal of Geology

## Filling the gap in the classification of phlogopite bearing ultramafic rocks

--Manuscript Draft--

<b>Manuscript Number:</b>	80760R1
<b>Full Title:</b>	Filling the gap in the classification of phlogopite bearing ultramafic rocks
<b>Article Type:</b>	Major Article
<b>Corresponding Author:</b>	Maurizio Mazzucchelli, M.D. Universita degli Studi di Modena e Reggio Emilia Modena, ITALY
<b>Corresponding Author Secondary Information:</b>	
<b>Corresponding Author's Institution:</b>	Universita degli Studi di Modena e Reggio Emilia
<b>Corresponding Author's Secondary Institution:</b>	
<b>First Author:</b>	Tommaso Giovanardi, Post doc fellow
<b>First Author Secondary Information:</b>	
<b>Order of Authors:</b>	Tommaso Giovanardi, Post doc fellow
	Ivan Freddo, Master Student
	Maurizio Mazzucchelli, M.D.
<b>Order of Authors Secondary Information:</b>	
<b>Manuscript Region of Origin:</b>	ITALY
<b>Abstract:</b>	<p>In recent years, the many new occurrences reported in the literature of ultramafic rocks with phlogopite as a major constituent and not falling into the category of Kimberlites, Lamproites and Lamprophyres, have highlighted the need of a classification that includes this abundant mineral phase. Currently, a broadly accepted classification with phlogopite does not exist and the only term used by scientists is 'bearing phlogopite' when this phase is above 5 Vol.% and up to 90 Vol.%. For this reason, we propose a new classification that integrates phlogopite into the current classification of ultramafic rocks, without modifying the already accepted terminology or the classificative criteria (i.e. the mineral modal abundances). Phlogopite is added as an end-member in the ultramafic rocks classification diagrams, changing their shapes from triangular to tetrahedral. An excel spreadsheet containing the new diagrams and a macro that automatically classifies the rocks is provided.</p>

# **Filling the gap in the classification of phlogopite bearing ultramafic rocks**

Giovanardi Tommaso<sup>1</sup>, Freddo Ivan<sup>1</sup>, Mazzucchelli Maurizio<sup>1</sup>

1 Dipartimento di Scienze Chimiche e Geologiche, Università degli Studi di Modena e Reggio Emilia, Via G. Campi, 103, 41125 Modena (Italy)

e-mail:

Giovanardi Tommaso: [tommaso.giovanardi@gmail.com](mailto:tommaso.giovanardi@gmail.com)

Freddo Ivan: [192748@studenti.unimore.it](mailto:192748@studenti.unimore.it)

Mazzucchelli Maurizio: [maurizio.mazzucchelli@unimore.it](mailto:maurizio.mazzucchelli@unimore.it)

## 1    **ABSTRACT**

2

3    In recent years, the many new occurrences reported in the literature of ultramafic rocks with  
4    phlogopite as a major constituent and not falling into the category of Kimberlites, Lamproites and  
5    Lamprophyres, have highlighted the need of a classification that includes this abundant mineral phase.  
6    Currently, a broadly accepted classification with phlogopite does not exist and the only term used by  
7    scientists is 'bearing phlogopite' when this phase is above 5 Vol.% and up to 90 Vol.%. For this  
8    reason, we propose a new classification that integrates phlogopite into the current classification of  
9    ultramafic rocks, without modifying the already accepted terminology or the classificative criteria  
10    (i.e. the mineral modal abundances). Phlogopite is added as an end-member in the ultramafic rocks  
11    classification diagrams, changing their shapes from triangular to tetrahedral. An excel spreadsheet  
12    containing the new diagrams and a macro that automatically classifies the rocks is provided.

13

14

## 15    **INTRODUCTION**

16

17    In many areas of the continental crust, the number of discoveries of ultramafic rocks rich in phlogopite  
18    that are different from Kimberlites, Lamproites and Lamprophyres has increased (Judd, 1885;  
19    Johannsen, 1938; Coteló Neiva, 1947; Dawson and Smith, 1977; Kramers et al., 1983; Meyer and  
20    Villa, 1984; Moreva, 1985; Szabó, 1985; Erlank et al. 1987; Sen, 1988; Neal and Taylor, 1989;  
21    Giannetti and Luhr, 1990; Lloyd et al., 1991; Ionov and Hofmann, 1995; Schumacher et al., 1996;  
22    Dessai and Vaselli, 1999; Zanetti et al., 1999, 2013, 2014, 2016; Richter and Elguera, 2001; Van  
23    Achterberg et al., 2001; Grégoire et al., 2002; Morishita et al., 2003, 2008; Downes et al., 2004a, b;  
24    Bell et al., 2005; Devaraju et al., 2006; Ho et al., 2006; Liu et al., 2011; Selverstone and Sharp, 2011;  
25    Fernando et al., 2013; Giovanardi et al., 2013, 2014; Vrijmoed et al., 2013; Bulchoz et al., 2014;  
26    Trubac et al., 2015; Kaczmarek et al., 2016). In these rocks, the term phlogopite is used not only to

point out the trioctahedral mica's Mg-endmember, but also to denote Mg-rich intermediate micas between the phlogopite and annite endmembers (down to  $Mg\# = 0.64$ , Ionov and Hofmann, 1995). In this article we will use the term phlogopite according to the biotite classification of Deer et al. (1966) which comprehends all the trioctahedral micas with  $Mg\# > 0.67$  (i.e. phlogopite and Fe-rich phlogopite). Some of the best examples of phlogopite bearing peridotites and pyroxenites outcrop in the Finero massif (Ivrea-Verbano Zone, Western Southern alps, Italy; Zanetti et al., 1999, 2013, 2014, 2016; Morishita et al., 2003, 2008; Selverstone and Sharp, 2011; Giovanardi et al., 2013, 2014). Other examples are given by mantle xenoliths entrapped in alkaline and high alkaline melts, like the so-called MARID (Mica-Amphibole-Rutile-Ilmenite-Diopside; Dawson and Smith, 1977), PP (Phlogopite-bearing Peridotites) and PKP (Phlogopite-K-richterite-bearing Peridotites; Erlank et al. 1987) and PIC rocks (Phlogopite-Ilmenite-Clinopyroxene-minor rutile; Grégoire et al., 2002) suites of xenoliths in kimberlites. In these cases, authors have commonly used acronyms to name the rocks. More frequently, the 'phlogopite-bearing' term is used in association with the current classification of ultramafics, thus not considering the % of phlogopite volume, which can vary from 5 % by Vol. up to 90 %. Moreover, the nomenclature reported in the literature to describe this type of rocks is rather obsolete and unused. For example, the term "Abessedite" indicates a variety of peridotite composed of olivine, hornblende and phlogopite (Cotelo Neiva, 1947, Abessédo Mine, Bragança district, Portugal), the name "Pikeite" denotes a phlogopite peridotite (Johannsen, 1938; Pike County, Arkansas, USA), or "Scyelite" that describes an olivine-hornblendite with phlogopite (Judd, 1885, Loch Scye, Scotland, UK). In few cases, phlogopite-rich rocks are known by local names as for the Finero area, where "Tomboghisinite" is a peridotite formed by phlogopite and olivine, "Föeradibalite" is a peridotite formed by olivine and hornblende and "Celhodurite" is a phlogopite and hornblende rich websterite (Zanetti et al., 1999; Zanetti, personal communication). Currently, the only attempt to classify Phl-rich rocks has been put forward by Szabó (1985), which has provided a specific classification system for ultramafic xenoliths with high phlogopite modal content found in Hungarian lamprophyric dikes. However, this classification does not include the

53 presence of both phlogopite and orthopyroxene (Szabó, 1985), which could coexist normally in  
54 ultramafic rocks (e.g. the phlogopite-bearing harzburgite in Finero; Zanetti et al., 1999 and others),  
55 thus leaving a major classification gap. Yet, there is no broadly accepted classification that considers  
56 phlogopite as a main mineral phase along with those most commonly contained in ultramafic rocks,  
57 that is olivine, orthopyroxene, clinopyroxene and hornblende.

58 The classification we propose uses a terminology that is not in conflict with the current classification  
59 of ultramafics accepted in the scientific community, but constitutes an extension. In addition, an excel  
60 spreadsheet (also compatible with Libreoffice and Openoffice) has been created to allow the practical  
61 use of the newly proposed diagrams. To demonstrate the functionality of the new classification, some  
62 ultramafic rock samples rich in phlogopite reported in the literature have been reclassified according  
63 to the new nomenclature.

## 64

## 65

## 66 **THE CURRENT IUGS ULTRAMAFIC ROCK CLASSIFICATION**

### 67

### 68 **The IUGS Recommendation**

### 69

70 The classification of ultramafic igneous rocks is carried out using the modal composition expressed  
71 as percentage by weight of the constituent minerals. The IUGS subcommission on the systematic of  
72 the igneous rocks suggests the use of two triangular diagrams designed by Streckeisen (1973). The  
73 first one is based on the modal proportion of olivine, orthopyroxene and clinopyroxene (Fig.s 1 and  
74 2). The second one is based on olivine, pyroxenes and hornblende (Fig.s 3 and 4), with M = mafic  
75 and related minerals, e.g. mica, amphibole, pyroxene, olivine, opaque minerals, accessory minerals  
76 (e.g. zircon, apatite, titanite), epidote, allanite, garnet, melilite, monticellite, primary carbonate >  
77 90%. With this method it is possible to distinguish three main groups of ultramafic rocks: 1)  
78 peridotites, formed by more than 40% of olivine and the rest of pyroxenes or amphibole (dunites with

79 more than 90% of olivine); 2) pyroxenites and 3) hornblendites, containing less than 40% olivine,  
80 mainly composed of either pyroxenes or amphiboles.

81 If the rocks contain less than or equal to 5% spinel, garnet, magnetite, chromite or phlogopite, this  
82 might be indicated by the addition of the word "with" after the name of the rock followed by that of  
83 the specific mineral (e.g. peridotite with garnet). However, more recently, it has become of common  
84 use to delete the "with" word and precede the rock name by the mineral name (e.g. garnet peridotite).

85

86

### 87 **Problems in the Classification of Rocks Rich in Phlogopite**

88

89 There are several examples in literature of findings of ultramafic rocks that, along with the most  
90 common phases such as olivine, pyroxene and amphibole, consist of non-negligible amounts of  
91 phlogopite, sometimes even more than 20%. An example is sample PC128 (Giannetti and Luhr, 1990)  
92 from the Roccamonfina volcano (Italy), whose modal composition includes Ol (8.6%), Cpx (63.1%),  
93 Phl (27.9%) and Sp (Trace) [1] or sample RGM319101 from Siebengebirge in Germany (Moreva,  
94 1985) formed by Ol (10%), Cpx (60%) and Phl (30%).

95 The lack of an appropriate classification, suitable for ultramafic rocks with phlogopite, triggers  
96 systematic anomalies in the nomenclature documented by cases in which the same name is given to  
97 rocks that have a significantly different composition. For example, sample FL19 of Lloyd et al.  
98 (1991), consisting of Cpx (44.5%), Phl (51.2%) and Sp (Trace), where the dominant mineral is  
99 phlogopite, is named phlogopite pyroxenite, but such is named also sample AY-506 from Righter and  
100 Elguera (2001) with Ol (1.7%), Cpx (57.6%), Phl (31.6%) and Ap (9.1%), where clinopyroxene is  
101 the most abundant mineral phase.

102 Conversely, we have encountered cases in the literature where the composition of two samples is very  
103 similar, but their nomenclature is different. For example, the A sample of Lloyd, (1985) consisting of  
104 Ol (Trace), Cpx (52.5%), Phl (37.0%) and Ap (1.0%), is named phlogopite clinopyroxenite, whereas

105 the LSC188 sample of Downes et al. (2004) made of Opx (6.0%), Cpx (54.4%), Phl (36.0%) is  
106 defined as mica websterite.

107 Another type of incongruity concerns rocks that are classified as peridotites when the percent  
108 recalculation is performed after removing phlogopite from the modal composition. This is the case of  
109 sample LSC240 of Downes et al. (2004) from Bearpaw Mountains in Montana (USA) consisting of  
110 Ol (32.2%), Opx (10.1%), Cpx (18.8%) and Phl (39%). If this sample is classified using the Ol-Opx-  
111 Cpx diagram of Streckeisen (1973), the recalculated modal composition results in Ol (52.8%), Opx  
112 (16.7%), Cpx (30.7%), corresponding to a lherzolite (Downes et al., 2004, classified the rock as a  
113 'mica lherzolite'), even though the original Ol content is less than 40%.

114

115

## 116 **THE CLASSIFICATION OF PHLOGOPITE BEARING ULTRAMAFIC ROCKS**

117

118 The basic idea for the new classification was to keep unchanged the nomenclature and classes  
119 proposed by Streckeisen (1973) for ultramafic rocks and only to integrate the missing phlogopite  
120 component. Moreover, we wanted to create a fairly intuitive classification with a nomenclature that  
121 takes upon the existing one.

122 Since the goal is to create a classification applicable to phlogopite-rich ultramafic rocks, we decided  
123 to implement the modal Ol-Opx-Cpx and Ol-Px-Hbl triangular diagrams adding the phlogopite. The  
124 two obtained systems have four phases each (Phl-Ol-Cpx-Opx and Phl-Ol-Px-Hbl) resulting in two  
125 tetrahedral diagrams, named POCO and POPH, respectively.

126 Both the inner volume and the outer faces of the tetrahedrons have been divided into fields.  
127 The bases of the tetrahedrons POCO and POPH correspond to the Streckeisen (1973) ternary  
128 diagrams Ol-Opx-Cpx and Ol-Px-Hbl, respectively, therefore the existing subdivisions have been  
129 applied.



130 The other faces represent new ternary diagrams for which we propose the following subdivisions. For  
131 the POCO tetrahedron, Ol-Phl-Cpx and Ol-Phl-Opx faces have been constructed with the fields of  
132 dunite ( $\text{Ol} > 90\%$ ), clinopyroxenite ( $\text{Cpx} > 90\%$ ), orthopyroxenite ( $\text{Opx} > 90\%$ ) and phlogopitite ( $\text{Phl} >$   
133  $90\%$ ) at the vertices. In literature there is no consensus on the name for rocks composed mainly by  
134 phlogopite: some authors prefer the old german term 'glimmerite' while others prefer to decline the  
135 mineral name using the -ite ending (i.e. phlogopitite) similar to pyroxene-rich rocks (i.e. pyroxen-ite,  
136 orthopyroxen-ite and clinopyroxen-ite). We have decided to use the phlogopitite term to follow the  
137 IUGS recommendations. According to the Streckeisen diagrams, a line corresponding to 40% olivine  
138 modal content and other lines corresponding to 5% of clinopyroxene, orthopyroxene, phlogopite, and  
139 olivine are plotted. Another segment connects the 50% on the Cpx-Phl and the Opx-Phl sides of the  
140 two diagrams with the dunite field.

141 The latter segment is also projected on the face Phl-Cpx-Opx to form the segment passing through  
142 50% of the phlogopite modal content. Likewise, on this face, the fields of orthopyroxenite,  
143 clinopyroxenite and phlogopitite have been outlined along with the segments for 5% modal content  
144 of each mineral.

145 The fields obtained in the four faces of the POCO tetrahedron mark different inner volumes in the  
146 solid diagram.

147 In order to easily determine the new nomenclature for the created fields, a set of all faces of the  
148 diagram can be obtained by "exploding" the tetrahedron into a flat shape (Fig. 1). Terms already  
149 established by the IUGS subcommission for the fields within the Streckeisen triangle have been  
150 maintained. The name "phlogopite dunite" indicates those rocks consisting mainly of these two  
151 minerals, with olivine over 40% and phlogopite less than 60%.

152 Specifically, the POCO tetrahedron is subdivided internally into various volumes (Fig. 2). For mineral  
153 abundances equal to 0%, the rock name is the one reported on the specific tetrahedron face.

154 Planes representing sums of two phases equal to 5% cut the tetrahedron edges and are truncated at  
155 the vertices by single-phase fields. The names of these internal solid volumes have been conceived

156 by generalizing those already used for the faces. The POCO internal volumes are: a) olivine and  
157 phlogopite websterite (less than 40% of Ol and more than 50% of Px), b) pyroxene and olivine  
158 phlogopitite (less than 40% of Ol and more than 50% of Phl), c) phlogopite lherzolite (more than 40%  
159 of Ol and more Px than Phl) and d) phlogopite and pyroxene dunite (more than 40% of Ol and more  
160 Phl than Px).

161 The POPH tetrahedron (Fig.s 3 and 4) has been constructed similarly to the POCO. However, it has  
162 been necessary to add an extra plane, which separates the “pyroxenite” and “hornblendite” fields, and  
163 extend it to the peridotite volume. In this diagram the name "hornblende dunite" indicates those rocks  
164 consisting mainly of these two minerals, with olivine over 40% and hornblende less than 60%.

165 Internal volumes in POPH are: a) pyroxene and hornblende phlogopitite (more than 50% of Phl, less  
166 than 40% of Ol and more Px than Hbl), b) hornblende and pyroxene phlogopitite (more than 50% of  
167 Phl, less than 40% of Ol and more Hbl than Px), c) phlogopite, pyroxene and olivine hornblendite  
168 (more than 50% of Hbl and less than 40% of Ol), d) phlogopite, hornblende and olivine websterite  
169 (more than 50% of Px and less than 40% of Ol), e) phlogopite, pyroxene and hornblende dunite (more  
170 than 40% of Ol, more Phl than the sum of Hbl and Px, and with more Px than Hbl), f) phlogopite,  
171 hornblende and pyroxene dunite (more than 40% of Ol, more Phl than the sum of Hbl and Px, and  
172 with more Hbl than Px), g) hornblende, phlogopite and pyroxene dunite (more than 40% of Ol, more  
173 Hbl than the sum of Phl and Px) and h) phlogopite and hornblende peridotite (more than 40% of Ol,  
174 more Px than the sum of Hbl and Phl).

175 The classificatory mineral phases present in minor modal proportion must be expressed according to  
176 their relative abundances: e.g. 'pyroxene and olivine phlogopitite' if the pyroxenes are more abundant  
177 than olivine or 'olivine and pyroxene phlogopitite' if the olivine is more abundant.

178

179

## 180 **THE EXTENSION OF THE ULTRAMAFIC ROCKS CLASSIFICATION**

181

182 The new tetrahedral classification has also been implemented to include both ortho- and  
183 clinopyroxene at the vertices of the diagram, combining the Ol-Opx-Cpx and Ol-Px-Hbl diagrams.  
184 This allows a more specific and accurate classification of samples. The diagram has been named  
185 COHO (Cpx-Opx-Hbl-Ol) and has the same subdivisions that have been described for the POCO  
186 tetrahedron (Fig.s 5 and 6).

187 Internal volumes (more than 5% of the sum of two phases and more than 0% of each phases) are: a)  
188 hornblende and olivine websterite (less than 40% of Ol, more than 50% of the sum of Cpx and Opx),  
189 b) pyroxene and olivine hornblendite (less than 40% of Ol, more Hbl than the sum of Cpx and Opx),  
190 c) hornblende lherzolite (more than 40% of Ol, sum of Cpx and Opx more than Hbl) and d)  
191 hornblende and pyroxene dunite (more than 40% of Ol, Hbl more than the sum of Cpx and Opx).

192 In summary, for each point of the various tetrahedrons, either on the faces or within their volumes,  
193 the sum of the four components is equal to 100. At each vertex, the presence of a specific mineral is  
194 100% and hence the remaining value is 0 %. If the sum of the modal percentages of the sample falls  
195 on a face the rock will assume the name of the field, if it falls within the tetrahedron the rock will be  
196 classified according to the name of the volumetric field in which it is located.

197 For amphibole higher than 5% and phlogopite less than 5%, the phlogopite is considered negligible  
198 and the classification can be made the COHO tetrahedron.

199 When the amount of phlogopite exceeds 5% and the presence of amphibole is less than 5%, the POCO  
200 tetrahedron comes into play. If both amphibole and phlogopite exceed 5% the POPH tetrahedron is  
201 used.

202

203

204 **CLASS-ULTRAMAFIC: A NEW SPREADSHEET FOR THE CLASSIFICATION OF**  
205 **ULTRAMAFIC ROCKS**

206

207 The best way to view the data within a tetrahedron is to use suitable software. We modified the Excel  
208 spreadsheet "Tetra-plot" (Cucciniello, 2016) based on a spreadsheet developed by Shimura and Kemp  
209 (2015) and applied several improvements.

210 The CLASS-ULTRAMAFIC Excel contains a calculation sheet and a diagram sheet of each  
211 tetrahedron: POCO, POPH and COHO. An "Instructions" sheet contains all the information to the use  
212 of the spreadsheet. The "input data" sheet contains a table of 18 columns and more than 1000 rows.  
213 In this sheet, the modal abundance in percent must be entered for each mineral found in the rock  
214 sample (symbols and text must be avoided). The data are automatically reported in each calculation  
215 sheet and evaluated by a function that determines the right classification to be used. Internal functions  
216 in the "Calculated data" sheets halt the classification in the not relevant sheets writing \*\*\* in column  
217 H and modifying the mineral abundances to 0%. The data in the proper classification sheet are then  
218 recalculated to 100% to apply the classification and transformed into x, y coordinates using  
219 trigonometric equations [1] and [2].

220

221 [1]  $Y' = X * \cos(\gamma * \pi / 180) * -\sin(\beta * \pi / 180) * -\sin(\alpha * \pi / 180) + \sin(\gamma * \pi / 180) * \cos(\alpha * \pi /$   
222  $180) + Y * \sin(\gamma * \pi / 180) * -\sin(\beta * \pi / 180) * -\sin(\alpha * \pi / 180) * \cos(\alpha * \pi / 180) + Z * \cos(\beta * \pi /$   
223  $\pi / 180) * -\sin(\alpha * \pi / 180)$

224

225 [2]  $X' = X * \cos(\beta * \pi / 180) * \cos(\gamma * \pi / 180) + Y * -\sin(\gamma * \pi / 180) * \cos(\alpha * \pi / 180) + Z * \sin$   
226  $(\beta * \pi / 180)$

227

228 where  $\gamma$ ,  $\alpha$  and  $\beta$  are the rotation angles of the tetrahedron visible in the "Tetrahedron" sheet in column  
229 B, rows 3,4 and 5.

230 The results of these calculations are shown in the table "Calculated Coordinates".

231 The "tetrahedron" sheet displays the tetrahedral diagram with the selected minerals at the vertices.  
232 Within the tetrahedron the planes are identified by different colors. Depending on the volume where  
233 the data falls, the sample name can be easily defined.  
234 The tetrahedron is able to rotate on the three axes x, y and z orthogonal to each other, in order to  
235 observe the position of the samples within the diagram. Angle values can be changed by moving the  
236 sliders of the three scroll bars in the upper left corner of the sheet. During the rotation, the position of  
237 the data and the planes remain solid with the tetrahedron.  
238 The spreadsheet is also equipped with a "classification macro", which automatically provides the rock  
239 name according to the new classification. The macro works only if column B (sample name) in the  
240 "Input Data" is filled. If the cell is filled the macro automatically tries to read the proper classification  
241 values in the "Calculated Data" sheet and inserts the rock name in column U (Classification) of the  
242 "Input Data" sheet. To start the macro the 'Classify' button must be clicked.  
243 The CLASS-ULTRAMAFIC is a .xlsx file and requires the software Excel 2007 or a newer version.  
244 The file also runs in Libreoffice and Openoffice permitting a completely free use of the spreadsheet,  
245 similar to few literature software (e.g., the Hf-INATOR; Giovanardi and Lugli, 2017). Within the  
246 spreadsheet, an exhaustive compilation of phlogopite-rich ultramafic rocks from literature is reported  
247 and classified.

248

249

## 250 **EXAMPLES BASED ON THE NEW CLASSIFICATION**

251

252 The new proposed classification for ultramafic rocks that includes phlogopite as a major end-member  
253 will be helpful to homogenize the currently extremely heterogeneous terminology for this kind of  
254 rocks.

255 Rocks with a non-negligible content of phlogopite will now have more appropriate names. Some  
256 examples are: sample RGM 319407 (Ol 85%, Phl 15%;) named dunite by Moreva (1985) and now

257 classified as phlogopite dunite, or sample WC253 (Ol 75.5%, Cpx 7%, Phl 16.7%;) named by Downes  
258 et al. (2004a) mica wehrlite and now re-named phlogopite and clinopyroxene dunite, or sample  
259 LSC241 (Ol 36%, Cpx 15.4%, Phl 48.5%;), named by Downes et al. (2004a) mica wehrlite and now  
260 classified as olivine and clinopyroxene phlogopitite.

261 Rocks with different compositions will now have different names as in the case of samples WC253  
262 and LSC241 reported above, or in the case of samples LSC238 (Ol 35.4% Cpx 15.9%, Phl 48.6;  
263 Downes et al., 2004a) and sample FL251 (Ol 44.3%, Cpx 41.5%, Phl 10.7%; Llyod et al., 1991),  
264 named both as mica wehrlite and now classified as olivine and clinopyroxene phlogopitite and  
265 phlogopite wehrlite respectively, or in the case of sample FL251 and FL4 (Ol 78.4%, Cpx 8.3%, Phl  
266 11.6%; Llyod et al., 1991), both named as mica wehrlite and now classified as phlogopite wehrlite  
267 and phlogopite and clinopyroxene dunite, respectively.

268 Conversely, rocks with similar mineralogical composition will have the same name: for example,  
269 samples JSL177-2 (Cpx 29%, Phl 67%; Lloyd, 1985) and LSC225 (Cpx 19.2%, Phl 80.8%; Downes  
270 et al., 2004a), named garnet phlogopite peridotite and mica clinopyroxenite respectively, are now  
271 classified as clinopyroxene phlogopitite.

272 The new classification also comes with a useful Excel spreadsheet already formatted and including a  
273 macro for automatic classification.

274

275

## 276 **ACKNOWLEDGEMENTS**

277

278 This work was supported by MIUR PRIN 2015 Prot.20158A9CBM\_005. We want to thank Riccardo  
279 Martoglia for help in the developing the Excel spreadsheet CLASS-ULTRAMAFIC and Anna  
280 Cipriani for the stimulating discussion. The Editor David B. Rowley and the two reviewers, Michel  
281 Gregoire and Claire Bucholz are also acknowledged for their useful comments which improved this  
282 work.

283   **REFERENCES**

284

285   Ahrens, L.H., Dawson J.B., Duncan A.R., and Erlank, A.J., 1973, Physics and chemistry of the Earth:  
286   Pergamon press, ISBN 0080180175, vol. 9, 940 p.

287   Bell, D.R., Gregoire, M., Grove, T.L., Chatterjee, N., Carlson, R.W., and Buseck, P.R., 2005, Silica  
288   and volatile-element metasomatism of Archean mantle: a xenolith-scale example from the Kaapvaal  
289   Craton: Contribution to Mineralogy and Petrology, no. 150, p. 251-267.

290   Cucciniello, C., 2016, Tetra-Plot: A Microsoft Excel spreadsheet to perform tetrahedral diagrams:  
291   Periodico di Mineralogia, no: 85(2), DOI: <http://dx.doi.org/10.2451/2016PM625>.

292   Bucholz, C.E., Jagoutz, O., Schmidt, M.W., and Sambuu, O., 2014, Phlogopite and clinopyroxene  
293   dominated fractional crystallization of an alkaline primitive melt: petrology and mineral chemistry of  
294   the Dariv Igneous Complex, western Mongolia: Contributions to Mineralogy and Petrology: no. 167,  
295   994, <https://doi.org/10.1007/s00410-014-0994-6>.

296   Deer, W.A., Howie, R.A., and Zussman, J., 1966, An introduction to the rock-forming minerals:  
297   Longman, London U.K.

298   Dessai, A.G., and Vaselli, O., 1999, Petrology and geochemistry of xenoliths in lamprophyres from  
299   the Deccan Traps: implications for the nature of the deep crust boundary in western India:  
300   Mineralogical Magazine, no. 63, p. 703-722.

301   Devaraju, T.C., Kaukonen, R.J., Sudhakara, T.L., and Alpiett, T.T., 2006, Tremolite-Olivine-  
302   Phlogopite-bearing Ultramafic Enclaves in the Archaean migmatite gneiss near Naregal, Gadag  
303   District, Karnataka: Journal of the Geological Society of India, no. 67, p. 312-316.

304   Downes, H., Beard, A., and Hinton, R., 2004, Natural experimental charges: an ion-microprobe study  
305   of trace element distribution coefficients in glassrich hornblende and clinopyroxenite xenoliths:  
306   Lithos, no. 75, p. 1-17.

307   Downes, H., Macdonald, R., Upton, B.G.J., Cox, K.G., Bodinier, J.L., Mason, P.R.D., James, D.,  
308   Hill, P.G., and Hearn, B.C., 2004, Ultramafic xenoliths from the Bearpaw Mountains, Montana, USA:

309 evidence for multiple metasomatic events in the lithospheric mantle beneath the Wyoming craton:  
 310 *Journal of Petrology*, no. 45, p. 1632-1662.

311 Fernando, G.W.A.R., Baumgartner, L.P., and Hofmeister, W., 2013, High-temperature  
 312 metasomatism of ultramafic granulites from the highland complex of Sri Lanka: *Journal of Geological*  
 313 *Society of Sri Lanka*, no. 15, p. 163-181.

314 Giannetti, B., and Luhr, J.F., 1990, Phlogopite-clinopyroxenite nodules from high-K magmas,  
 315 Roccamonfina Volcano, Italy: evidence for a low-pressure metasomatic origin: *Earth and Planetary*  
 316 *Science Letters*, no. 101, p. 404-424.

317 Giovanardi, T., Morishita, T., Zanetti, A., Mazzucchelli, M., and Vannucci R., 2013, Igneous  
 318 sapphirine as a product of melt-peridotite interactions in the Finero phlogopite–peridotite massif,  
 319 western Italian Alps: *European Journal of Mineralogy*, no 25, p. 17–31.

320 Giovanardi, T., Mazzucchelli, M., Zanetti, A., Langone, A., Tiepolo, M., and Cipriani, A., 2014,  
 321 Occurrence of phlogopite in the Finero mafic layered complex: *Open Geosciences*, no. 6(4), p. 588–  
 322 613.

323 Giovanardi, T., and Lugli, F., 2017, The Hf-INATOR: A free data reduction spreadsheet for Lu/Hf  
 324 isotope analysis: *Earth Science Informatics*, on-line published, DOI 10.1007/s12145-017-0303-9.

325 Grégoire, M., Bell, D.R., and LeRoex, A.P., 2002, Trace element geochemistry of phlogopite-rich  
 326 mafic mantle xenoliths: their classification and their relationship to phlogopite-bearing peridotites and  
 327 kimberlites revisited: *Contribution to Mineralogy and Petrology*, no. 144, p. 603-625.

328 Ho, K.S., Chen, J.C., and Chung, S.H., 2006, Composite mantle xenoliths in basaltic pyroclastic rocks  
 329 from Tungchihsu, Penghu Islands, Taiwan strait: evidence for a metasomatized lithospheric mantle  
 330 beneath SE China: *Collection and Research*, no. 19, p. 49-76.

331 Ionov, D.A., and Hofmann, A.W., 1995, Nb-Ta-rich mantle amphiboles and micas: Implications for  
 332 subduction-related metasomatic trace element fractionations: *Earth and Planetary Science Letters*, no.  
 333 131, p. 341-356.



334 Kaczmarek, M.A., Bodinier, J.L., Bosch, D., Tommasi, A., Dautria, J.M., and Kechid, S.A., 2016,  
 335 Metasomatized Mantle xenoliths as a record of the lithospheric mantle evolution of the northern edge  
 336 of the Ahaggar Swell, In Teria (Algeria): *Journal of Petrology*, no. 57, p. 345-382.  
 337 Kramers, J.D., Riddick, J.C.M., and Dawson, J.B., 1983, Trace element and isotope studies on veined,  
 338 metasomatic and "MARID" xenoliths from Bultfontein, South Africa: *Earth and Planetary Science*  
 339 *Letters*, no. 65, p. 90-106.  
 340 Liu, S.A., Teng, F.Z., Yang, W., and Wu, F.Y., 2011, High-temperature inter-mineral magnesium  
 341 isotope fractionation in mantle xenoliths from the north China craton: *Earth and Planetary Science*  
 342 *Letters*, no. 308, p. 131-140.  
 343 Lloyd, F.E., Edgar, A.D., Forsyth, M., and Barnett, R.L., 1991, The paragenesis of upper-mantle  
 344 xenoliths from the Quaternary volcanics southeast of Gees, West Eifel, Germany: *Mineralogical*  
 345 *Magazine*, no. 55, p. 95-112.  
 346 Meyer, H.O.A., and Villar, L.M., 1984, An alnoite in the Sierras Subandinas, Northern Argentina:  
 347 *Journal of Petrology*, no. 92, p. 741-751.  
 348 Moreva-Perekalina, T.V., 1985, Ultramafic xenoliths from alkaline basalts of Finkenberg  
 349 (Siebengebirge, West Germany): *Scripta Geologica*, no. 78, p. 1-65.  
 350 Morishita, T., Arai, S., and Tamura, A., 2003, Petrology of an apatite-rich layer in the Finero  
 351 phlogopite–peridotite, Italian Western Alps: implications for evolution of a metasomatising agent:  
 352 *Lithos*, no. 69, p. 37–49.  
 353 Morishita, T., Hattori, K.H., Terada, K., Matsumoto, T., Yamamoto, K., Takebe, M., Ishida, Y.,  
 354 Tamura, A., and Arai, S., 2008, Geochemistry of apatite-rich layers in the Finero phlogopite–  
 355 peridotite massif (Italian Western Alps) and ionmicroprobe dating of apatite: *Chemical Geology*, no.  
 356 251, p. 99–111.  
 357 Neal, C.R., and Taylor, L.A., 1989, The petrography and composition of phlogopite micas from the  
 358 Blue Ball Kimberlite, Arkansas: a record of chemical evolution during crystallization: *Mineralogy*  
 359 *and Petrology*, no. 40, p. 207-224.

360 Righter, K., and Elguera, J.R., 2001, Alkaline lavas in the volcanic front of the western mexican  
 361 volcanic belt: geology and petrology of the Ayutla and Tapalpa volcanic fields: *Journal of Petrology*,  
 362 no. 42, p. 2333-2361.

363 Schumacher, U.M., Keller, J., Kononova, V.A., and Suddaby, P.J., 1996, Mineral chemistry and  
 364 geochronology of the potassic alkaline ultramafic Inagli complex, Aldan Shield, eastern Siberia:  
 365 *Mineralogical Magazine*, no. 60, p. 711-730.

366 Sen, G., 1988, Petrogenesis of spinel Iherzolite and pyroxenite suite xenoliths from the Koolau shield,  
 367 Oahu, Hawaii: Implications for petrology of the post-eruptive lithosphere beneath Oahu: *Contribution*  
 368 *to Mineralogy and Petrology*, no. 100, p. 61-91.

369 Trubac, J., Vràna, S., Holuzová, E., and Ackerman, L., 2015, Petrology and geochemical  
 370 characteristics of phlogopite pyroxenite related to durbachites, Moldanubian Zone, Bohemian Massif:  
 371 *Journal of Geosciences*, no. 60, p. 73-90.

372 Van Achterberg, E., Griffin, W.L., and Stiefenhofer, J., 2001, Metasomatism in mantle xenoliths from  
 373 the Lethlakane kimberlites: estimation of element fluxes: *Contribution to Mineralogy and Petrology*,  
 374 no. 141, p. 307-414.

375 Vrijmoed, J. C., Austrheim, H., John, T., Hin, R.C., Corfu, F., and Davies, G.R., 2013, Metasomatism  
 376 in the ultrahigh-pressure Svartberget garnet-peridotite (Western Gneiss Region, Norway):  
 377 Implications for the transport of crust-derived fluids within the mantle: *Journal of Petrology*, no. 54,  
 378 p. 1815-1848.

379 Zanetti, A., Mazzucchelli, M., Rivalenti, G., and Vannucci, R., 1999, The Finero phlogopite-  
 380 peridotite massif: an example of subduction-related metasomatism: *Contribution to Mineralogy and*  
 381 *Petrology*, no. 134, p. 107-122.

382 Zanetti, A., Mazzucchelli, M., Sinigoi, S., Giovanardi, T., Peressini, G., and Fanning, M., 2013,  
 383 SHRIMP U–Pb zircon Triassic intrusion age of the Finero mafic complex (Ivrea–Verbano Zone,  
 384 Western Alps) and its geodynamic implications: *Journal of Petrology*, no. 54, p. 2225–2265.

385 Zanetti, A., Mazzucchelli, M., Sinigoi, S., Giovanardi, T., Peressini, G., and Fanning, M., 2014,  
386 SHRIMP U–Pb zircon Triassic intrusion age of the Finero mafic complex (Ivrea–Verbano Zone,  
387 Western Alps) and its geodynamic implications: *Journal of Petrology*, no. 55, p. 1239–1240.  
388 Zanetti, A., Giovanardi, T., Langone, A., Tiepolo, M., Wu, F.-Y., Dallai, L., and Mazzucchelli, M.,  
389 2016, Origin and age of zircon-bearing chromitite layers from the Finero phlogopite peridotite (Ivrea–  
390 Verbano Zone, Western Alps) and geodynamic consequences: *Lithos*, no. 262, p. 58–74.

391 **FIGURE CAPTIONS**

392

393 Fig. 1: 'exploded' faces of the POCO (Phl-Ol-Cpx-Opx) diagram and nomenclature.

394

395 Fig. 2: the POCO (Phl-Ol-Cpx-Opx) diagram (A) and its internal volumes: B) phlogopite and  
396 pyroxene / dunite; C) phlogopite lherzolite; D) pyroxene and olivine / phlogopite and E) olivine and  
397 phlogopite / websterites. The order of the minor abundant phases is fixed for convenience. Authors  
398 must change the terms order based on the relatively abundances of the phases (e.g. phlogopite and  
399 olivine websterite if the phlogopite is more abundant than olivine).

400

401 Fig. 3: 'exploded' faces of the POPH (Phl-Ol-Px-Hbl) diagram and nomenclature.

402

403 Fig. 4: the POPH (Phl-Ol-Px-Hbl) diagram (A) and its internal volumes of: B) phlogopite, hornblende  
404 and pyroxene dunite; C) phlogopite, pyroxene and hornblende dunite; D) hornblende, phlogopite and  
405 pyroxene dunite; E) phlogopite and hornblende / peridotite; F) hornblende, pyroxene and olivine /  
406 phlogopite; G) pyroxene, hornblende and olivine / phlogopite; H) phlogopite, pyroxene and olivine  
407 / hornblende and I) phlogopite, hornblende and olivine / websterite. The order of the minor abundant  
408 phases is fixed for convenience. Authors must change the terms order based on the relatively  
409 abundances of the phases (e.g. phlogopite and hornblende peridotite if the phlogopite is more  
410 abundant than hornblende).

411

412 Fig. 5: 'exploded' faces of the COHO (Cpx-Opx-Hbl-Ol) diagram and nomenclature.

413

414 Fig. 6: the COHO (Cpx-Opx-Hbl-Ol) diagram (A) and its internal volumes: B) hornblende and  
415 pyroxene / dunite; C) hornblende lherzolite; D) pyroxene and olivine / hornblende and E) olivine  
416 and hornblende / websterites;. The order of the minor abundant phases is fixed for convenience.

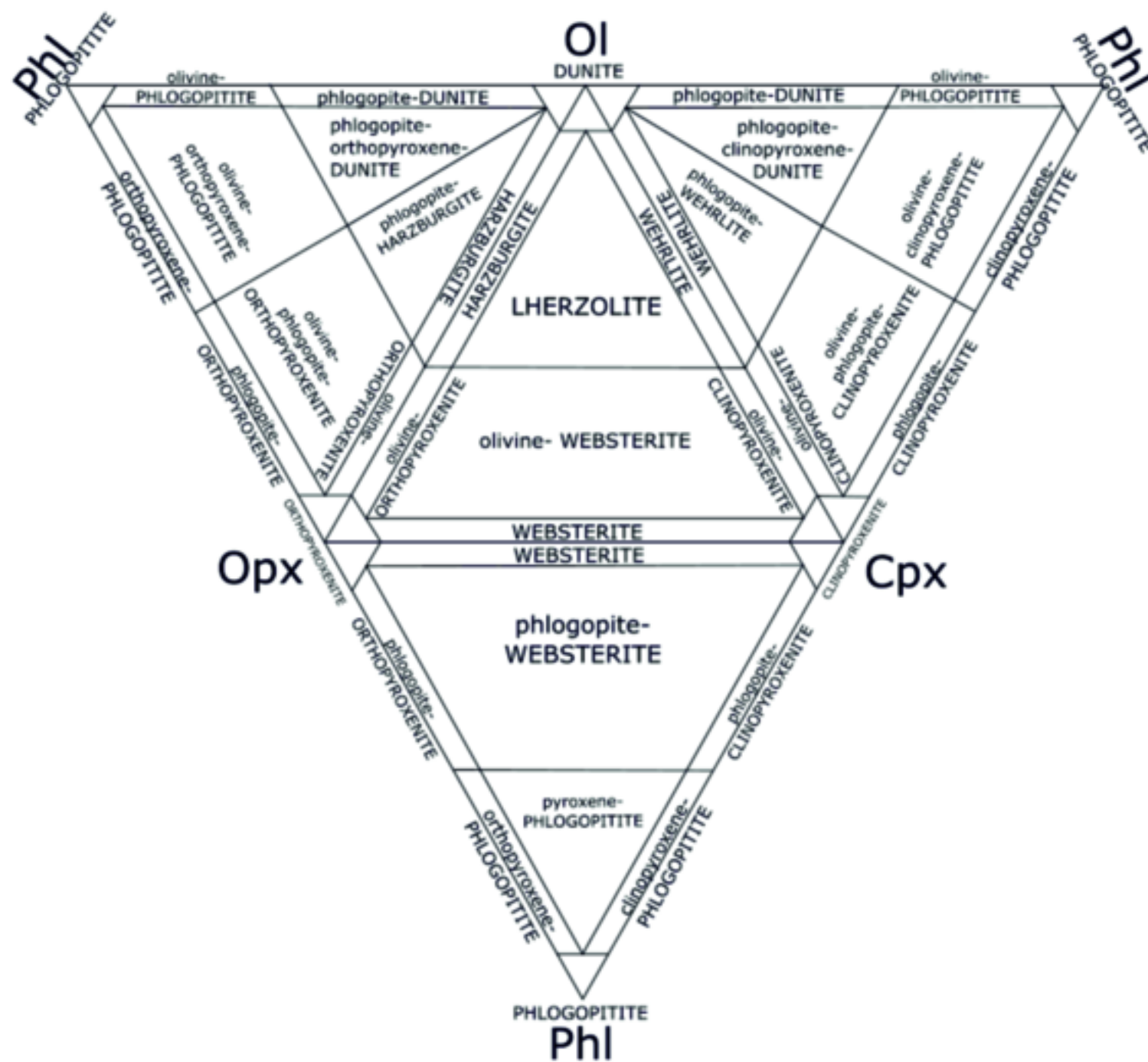
417 Authors must change the terms order based on the relatively abundances of the phases (e.g. pyroxene  
418 and olivine hornblendite if the pyroxene is more abundant than olivine).

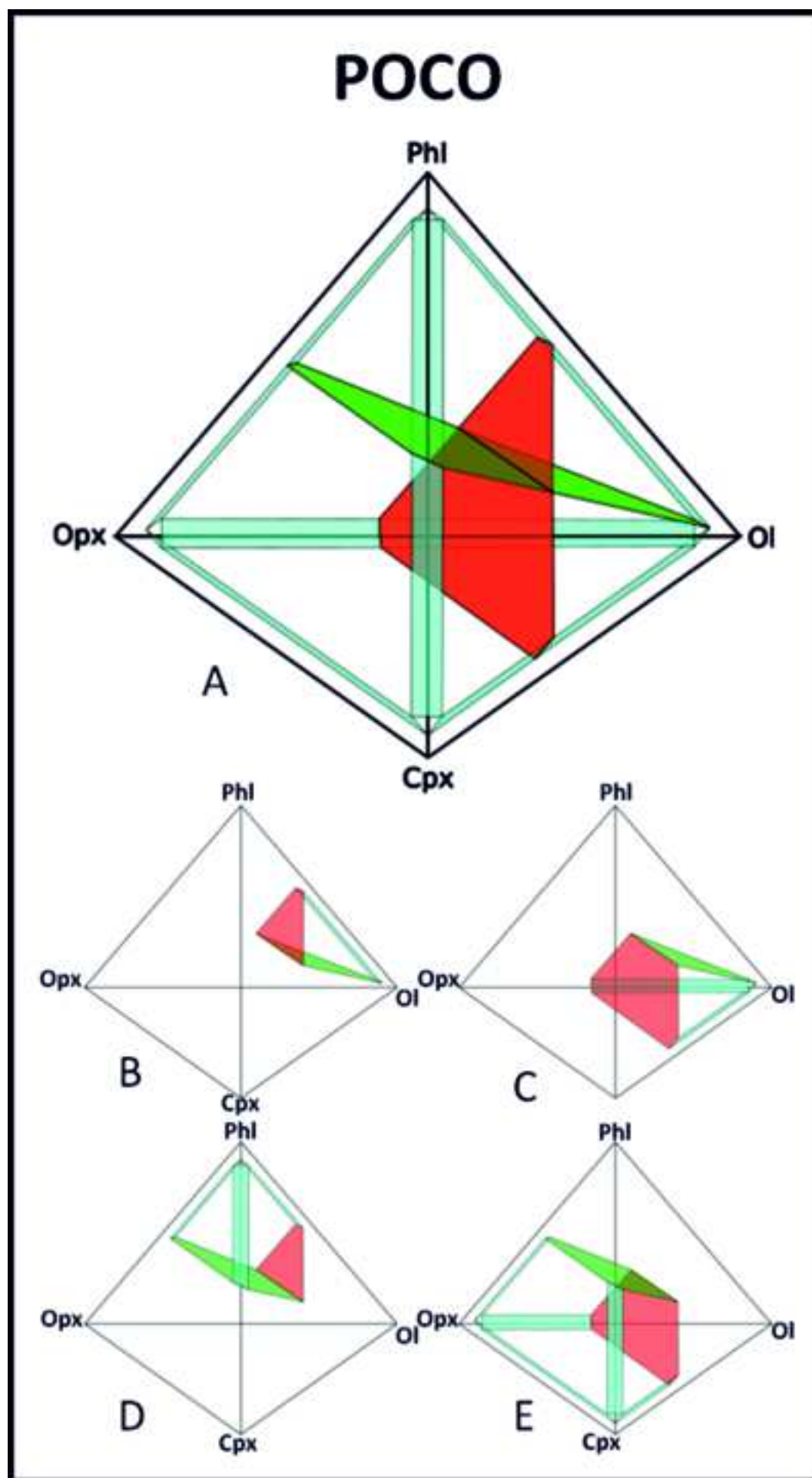
419

420 **Footnotes**

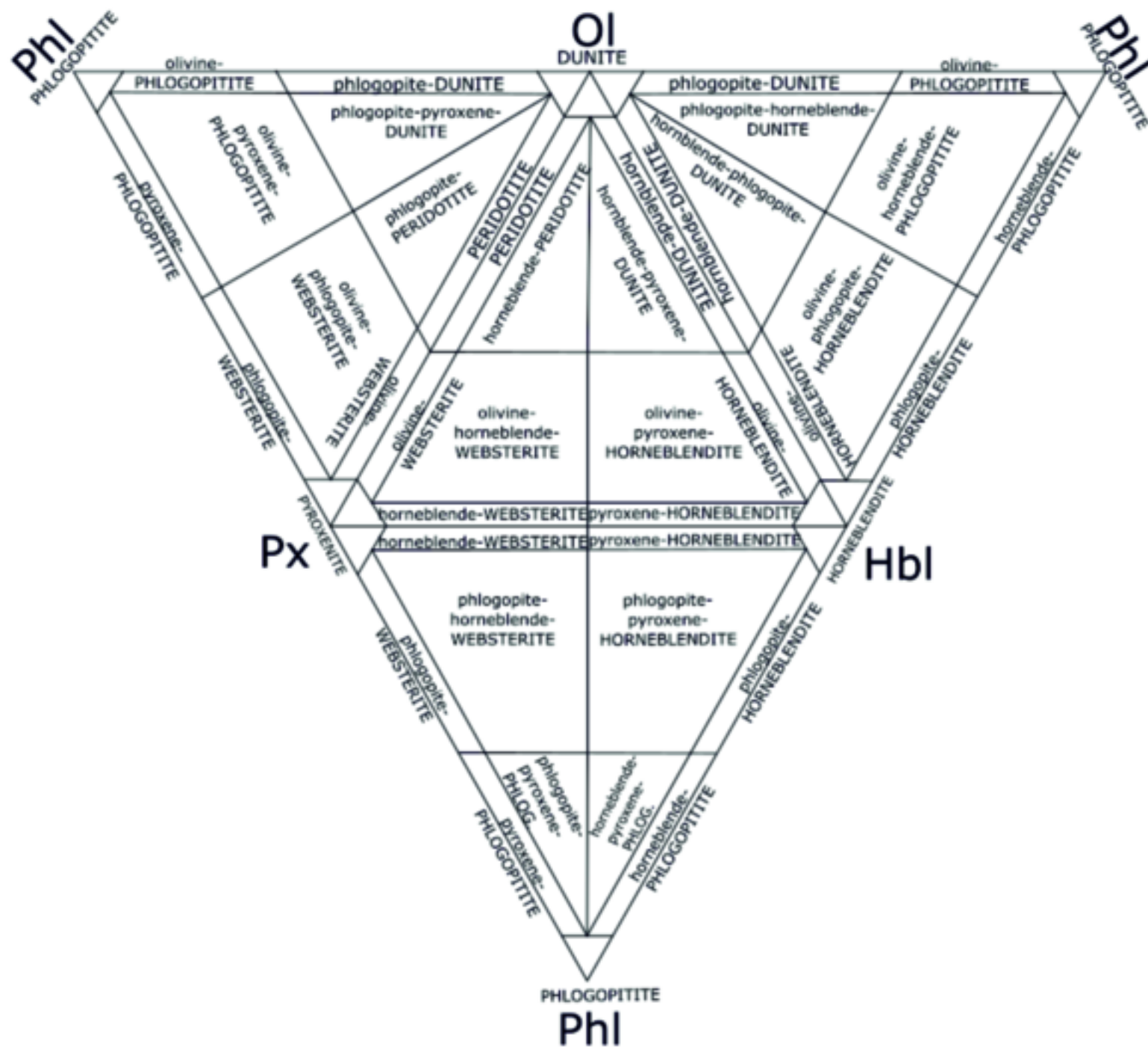
421 [1]: in this article mineral acronyms are used to report mineral modal compositions of rocks. The used  
422 acronyms are: Apatite, Ap; Clinopyroxene, Cpx; Hornblende, Hbl; Olivine, Ol; Orthopyroxene, Opx;  
423 Phlogopite, Phl; Pyroxenes, Px; Spinel, Sp.

[Click here to download Figure Fig 1.tif](#) 

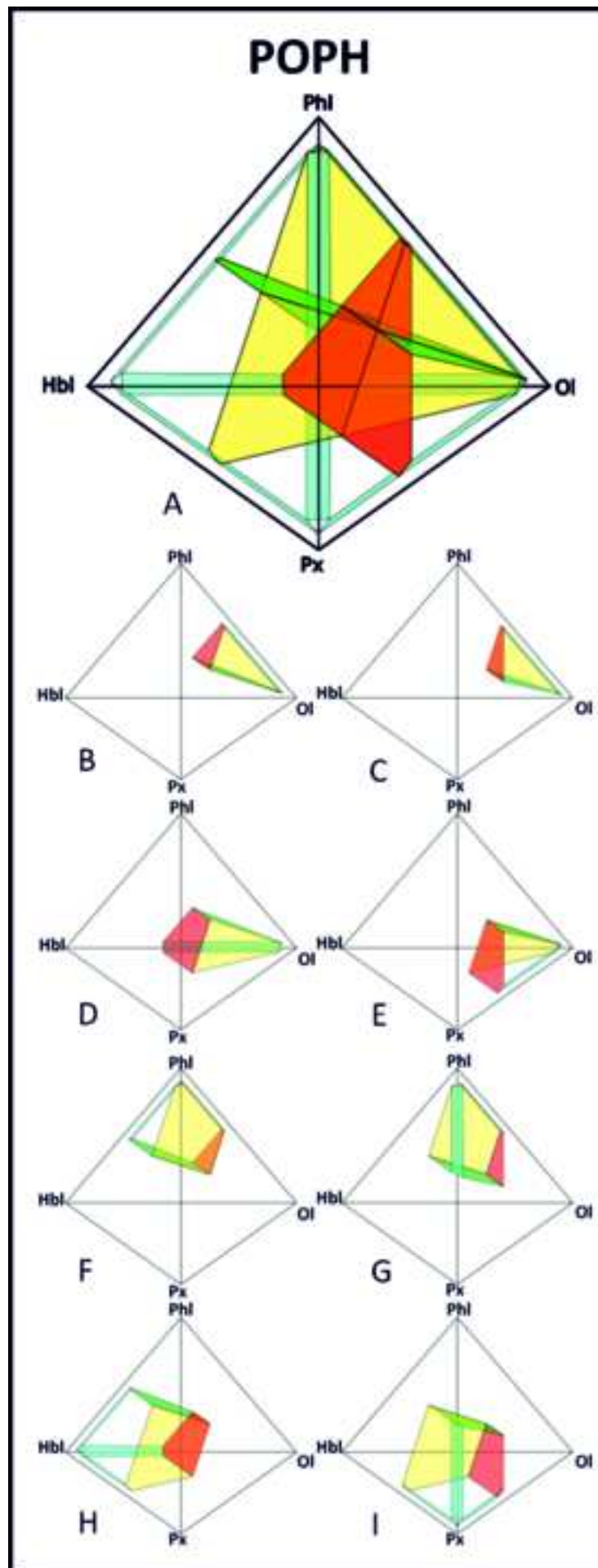




[Click here to download Figure Fig 3.tif](#) 







[Click here to download Figure Fig 5.tif](#) 

